ACCOUNTS
of chemical research

The Induced Magnetic Field

RAFAEL ISLAS,[†] THOMAS HEINE,[*,‡] AND GABRIEL MERINO[*,†]

[†]*Departamento de Química, Universidad de Guanajuato, Noria Alta s/n C.P. 36050, Guanajuato, Gto. México, and* [‡]*School of Engineering and Science, Jacobs University Bremen, 28759 Bremen, Germany*

RECEIVED ON MAY 14, 2011

CONSPECTUS

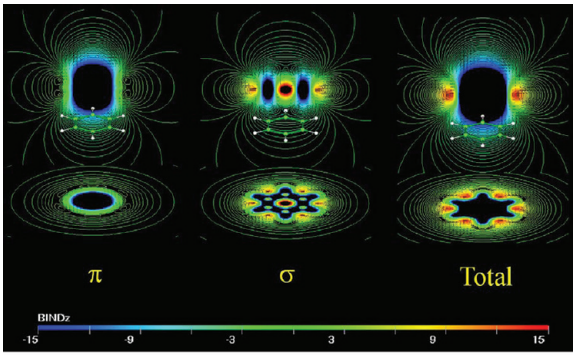

The z-component of $\mathbf{B}^{ind}$ of benzene

Aromaticity is indispensable for explaining a variety of chemical behaviors, including reactivity, structural features, relative energetic stabilities, and spectroscopic properties. When interpreted as the spatial delocalization of π-electrons, it represents the driving force for the stabilization of many planar molecular structures. A delocalized electron system is sensitive to an external magnetic field; it responds with an induced magnetic field having a particularly long range. The shape of the induced magnetic field reflects the size and strength of the system of delocalized electrons and can have a large influence on neighboring molecules.

In 2004, we proposed using the induced magnetic field as a means of estimating the degree of electron delocalization and aromaticity in planar as well as in nonplanar molecules. We have since tested the method on aromatic, antiaromatic, and nonaromatic compounds, and a refinement now allows the individual treatment of core-, σ-, and π-electrons.

In this Account, we describe the use of the induced magnetic field as an analytical probe for electron delocalization and its application to a large series of uncommon molecules. The compounds include borazine; all-metal aromatic systems Al_4^{n-}; molecular stars $Si_5Li_n^{6-n}$; electronically stabilized planar tetracoordinate carbon; planar hypercoordinate atoms inside boron wheels; and planar boron wheels with fluxional internal boron cluster moieties. In all cases, we have observed that planar structures show a high degree of electron delocalization in the π-electrons and, in some examples, also in the σ-framework.

Quantitatively, the induced magnetic field has contributions from the entire electronic system of a molecule, but at long range the contributions arising from the delocalized electronic π-system dominate. The induced magnetic field can only indirectly be confirmed by experiment, for example, through intermolecular contributions to NMR chemical shifts. We show that calculating the induced field is a useful method for understanding any planar organic or inorganic system, as it corresponds to the intuitive Pople model for explaining the anomalous proton chemical shifts in aromatic molecules. Indeed, aromatic, antiaromatic, and nonaromatic molecules show differing responses to an external field; that is, they reduce, augment, or do not affect the external field at long range. The induced field can be dissected into different orbital contributions, in the same way that the nucleus-independent chemical shift or the shielding function can be separated into component contributions. The result is a versatile tool that is particularly useful in the analysis of planar, densely packed systems with strong orbital contributions directly atop individual atoms.

Published on the Web 08/17/2011 www.pubs.acs.org/accounts
10.1021/ar200117a

Introduction

Ask freshman chemistry students to name one aromatic compound. Benzene, for sure, will be the most popular one. Now, ask them what is aromaticity? In this case, the answers could be so dissimilar. Like the chemical bond or electronegativity, aromaticity is only a concept, a fuzzy concept to explain the chemical properties of a series of compounds. Thus, as any *unicorn* in chemistry, its definition is neither simple nor free of controversy.[1] The IUPAC defines aromaticity as *"The concept of spatial and electronic structure of cyclic molecular systems displaying the effects of cyclic electron delocalization which provide for their enhanced thermodynamic stability (relative to acyclic structural analogues) and tendency to retain the structural type in the course of chemical transformations."*[2] In general, a quantitative and/or qualitative assessment of the aromaticity degree is given by chemical behavior (lower reactivity), structural features (planarity and equal bond length tendencies), energy (stability), and spectroscopic properties (UV, proton chemical shifts, magnetic susceptibility exaltation). Particularly, the magnetic properties have been employed to assess aromaticity, and several magnetic indexes have been introduced and discussed.[3,4] They include the famous nucleus-independent chemical shift (NICS) and related indexes,[5−7] aromatic ring-current shielding (ARCS),[8] and plotted ring-current densities.[9−12]

Quantum mechanics, even in the crudest approximation as formulated in Hückel theory,[13] is suitable for explaining the π-aromaticity. Application of this theory clarifies the planarity and stability of benzene and leads to the well-known $(4n + 2)\pi$-electrons rule for annulenes. The delocalized π-electrons affect not only the structure (planarity and high-symmetry) and enhanced stability of aromatic systems; they also determine their magnetic properties. For instance, the downfield value of the proton NMR chemical shift of benzene, compared to sp^2 carbon, has been rationalized by Pople[14] using a ring current model. In 1956, he stated that proton magnetic resonance of hydrocarbons can be better understood in terms of a more detailed picture of the diamagnetic current set up in the molecule by an external field. An external magnetic field ($\mathbf{B}^{ext}$), applied perpendicular to the ring, will, following Biot-Savart's law, produce a ring current which itself induces a counterfield. This law is valid for static magnetic fields and results in a $\mathbf{B}$ field consistent with both Ampère's law and Gauss's law for magnetism. In this sense, the magnetic response (the induced magnetic field, $\mathbf{B}^{ind}$) of any molecule will be a consequence of its electronic properties. So, it has sense to expect special magnetic response for an aromatic system, revealing important information on electron delocalization and, furthermore, of its origin. In 2004, we visualized the induced magnetic field in classical aromatic and antiaromatic molecules,[15] and in 2007 we illustrated the Pople model employing this tool to the π-system of these molecules.[16] Thenceforth, we have applied this tool in several systems in order to understand aromaticity and electron delocalization. Here, we review these contributions.

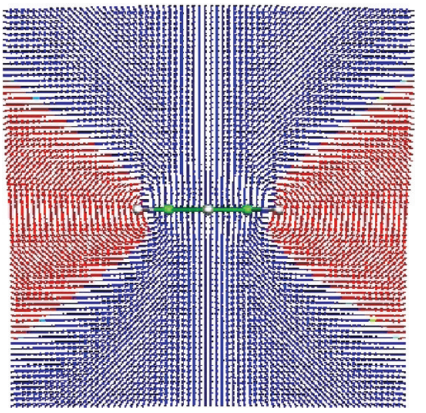

FIGURE 1. $\mathbf{B}^{ind}$ of benzene. The molecular ring lies in the *xy* plane of the Cartesian coordinates. The external magnetic field is applied in the *z*-axis direction, across the ring center. Red zones show paratropic regions around the molecule. Blue ones show diatropic zones.

Induced Magnetic Field

Induced fields are used by physicists and engineers to describe the magnetism of macroscopic devices, but also by chemists to understand the magnetic properties of molecules. Related quantities of electrodynamics, such as material constants, are accessible through $\mathbf{B}^{ind}$ and Maxwell's equations. $\mathbf{B}^{ind}$ is related to the shielding tensor at position $\mathbf{r}$ and the homogeneous external magnetic field $\mathbf{B}^{ext}$, eq 1.

$$\mathbf{B}^{ind}(\mathbf{r}) = -\sigma(\mathbf{r})\mathbf{B}^{ext} \quad (1)$$

Equation 1 does not contain information about nuclei, and hence, the shielding tensor can be computed anywhere in space, that is, at the position of a nucleus or somewhere else.[17] As the shielding tensor can be computed as expectation value from the wave function and is available by means of most recent quantum-chemistry programs at any level of theory, this approach is very practical for applications.

A magnetic field perpendicular to a plane containing free charge carriers induces a current density. This current density induces a counter field (Figure 1). In this sense, the induced magnetic fields and induced current densities are complementary to each other. Induced current densities

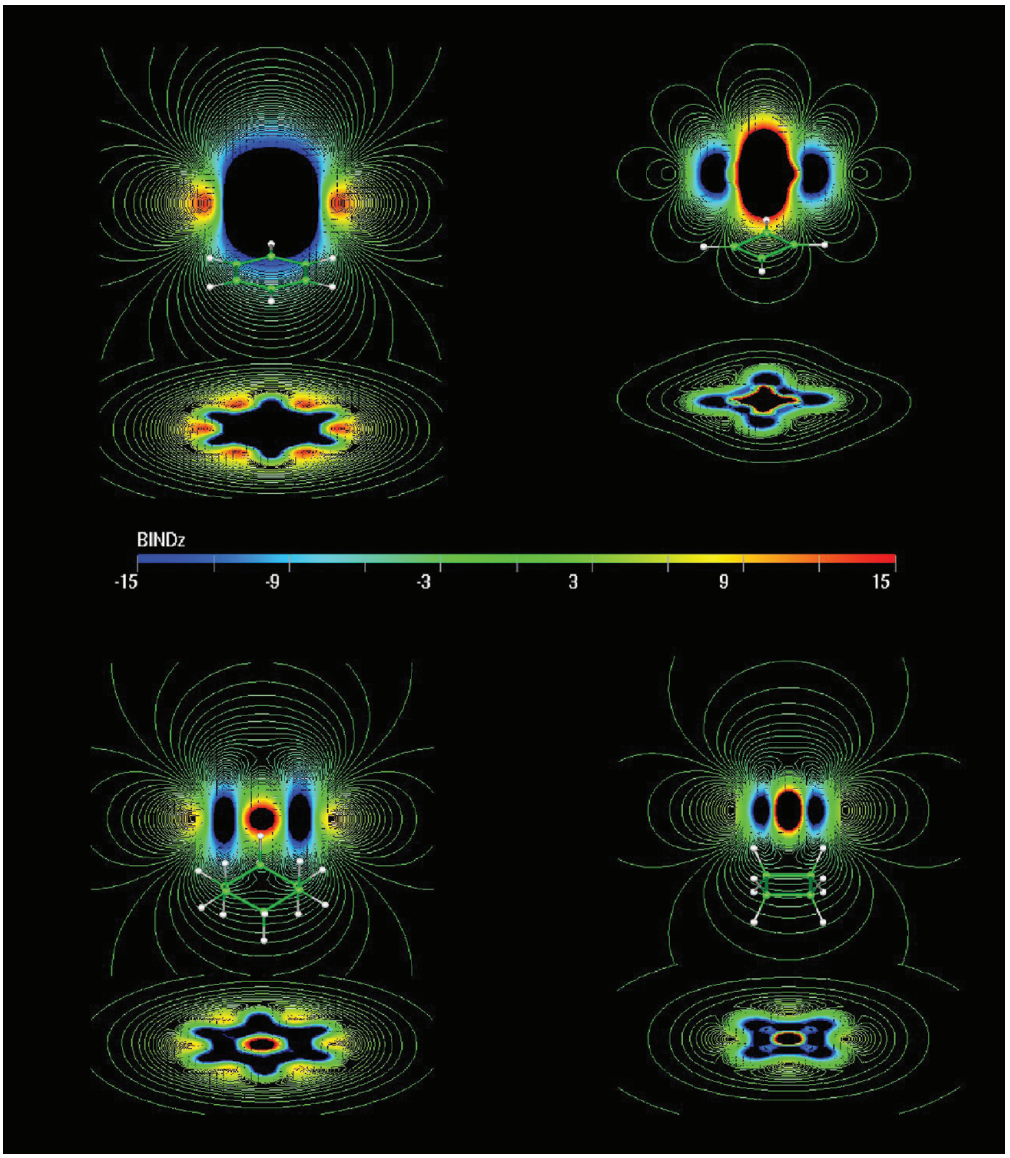

FIGURE 2. B^{ind}_z of benzene, cyclobutadiene, cyclohexane, and cyclobutane. Red zones show paratropic (deshielding) regions around the molecule. Blue ones show diatropic (shielding) zones. The induced magnetic field is given in ppm, which is equivalent to μT. $\mathbf{B}^{ind}$ computations were performed at the PW91/IGLO-III level.

are usually given in a selected plane parallel to the molecular ring, while the induced field contains information of the overall current density distribution. However, it is not clear whether $\mathbf{B}^{ind}$ originates solely from a ring current or not. Having both analyses available is, therefore, advantageous. In agreement with current–density maps, the response of aromatic, antiaromatic, and nonaromatic examples shows characteristic features.

Note that B^{ind}_z for an external field perpendicular to the ring is equivalent to σ_{33} (33 component of the shielding tenso) or the $NICS_{zz}$.[17,18] Usually, the *x* and *y* components of the induced magnetic field have nodes in the ring plane and parallel to the *z*-axis, but they do not have as long a range as the B^{ind}_z.

Benzene versus Cyclobutadiene

Nonconjugated systems, such as cyclobutane or cyclohexane, only show a short-range response to the magnetic field.[15] In all areas of the molecule, except for the immediate vicinity of atoms and bonds, the *z*-component of $\mathbf{B}^{ind}$ (B^{ind}_z) is small (Figure 2). This is different for conjugated rings: Both cyclobutadiene and benzene show magnetic fields far away from the molecule and significant contributions in the ring centers. However, the induced fields are either in line with the applied field, hence increasing it (paratropic) for antiaromatic compounds or shielding it (diatropic) for aromatic compounds. These trends are in agreement with the results of Schleyer et al., obtained by using NICS grids on top of the rings.[19]

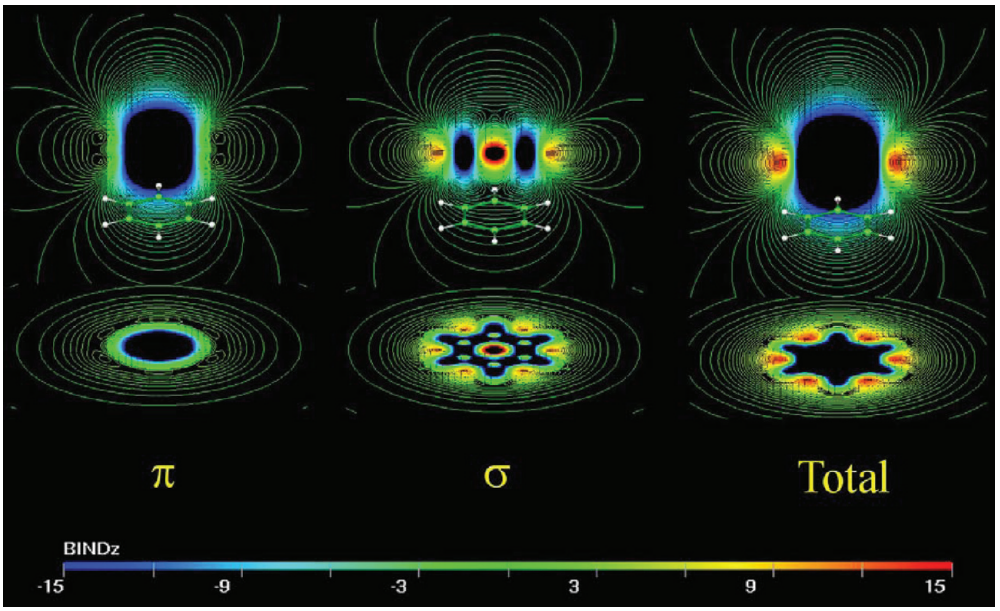

FIGURE 3. $B^{ind}{}_z$ of benzene. Blue and red areas denote diatropic and paratropic regions, respectively. $\mathbf{B}^{ind}$ computations were performed at the PW91/IGLO-III level.

Figure 2 also shows that above and below the ring the response of the molecule to the magnetic field is long-ranged for aromatic and antiaromatic molecules (though different in sign), while the σ-system is always surrounded by a diatropic region, and it is not dependent if the system is aromatic, antiaromatic, or nonaromatic. Contrary, aromatic and antiaromatic rings influence their surroundings through long-ranged magnetic fields and affect chemical shifts of surrounding nuclei. Note that $B^{ind}{}_z$ for an external field perpendicular to the ring is equivalent to the $NICS_{zz}$.[17] They have nodes in the ring plane and parallel to the *z*-axis and do not have as long a range as the $B^{ind}{}_z$ component.

Interestingly, the hydrogen atoms in benzene are located outside the vortexes of the induced field (see Figure 2) and inside the shielding rather than the deshielding region. A nodal ring, which separates the shielding from the deshielding region, encircles the molecule outside the hydrogen atoms. This observation opposes popular textbook explanations of abnormal ^{1}H NMR chemical shifts of aromatic molecules. However, the ring current model considers only ring currents arising from the π-cloud, and the discussed results also include the contributions from the σ-framework. The benzene response to a $\mathbf{B}^{ext}$ parallel to the molecular plane is of entirely different character than when the field is applied perpendicular to the ring; we observe short-range diatropic response parallel to the external field.[15] Also for the other components, the response is limited to the region around the σ-framework. Combining the results, we concluded that, at long range, the magnitude of the induced magnetic field is governed by its *z*-component.

Orbital Contributions to Induced Magnetic Field

Recently, the local contributions from the σ C−H and C−C bonds to the ring current effects have been subject of a controversial debate.[20,21] The current density and the induced field of a molecule are molecular vector fields correlated through Biot−Savart's law. In the Pople model,[14] and also in Lazzeretti's refinement,[11] only a ring current, projected out of the current density, is discussed. Ring currents have been calculated using several methods and models,[9,11] and it is well-established that a diatropic net ring current of benzene is caused by the π-electrons. The $\mathbf{B}^{ind}$ visualization for benzene shows that the protons lie in the shielding cone of benzene if the external field is applied perpendicular to the ring, which may lead to misinterpretations of Pople's model.[15] For the correct interpretation, the shielding contributions arising from the σ-framework need to be excluded from quantum chemical calculations.[22] Thus, to recover this model, it is necessary to calculate $\mathbf{B}^{ind}$ arising from the π-orbital contributions only. As our method allows the separation into σ- and π-orbitals, we can discuss the role of these contributions.[16] In benzene, the σ-orbital contributions to $\mathbf{B}^{ind}$ have a shape quite similar to the total $\mathbf{B}^{ind}$ of nonaromatic molecules.[15] As σ-electrons are much stronger localized than π-electrons, their local paramagnetic contributions generate a short-range response and a paratropic region in the center of the ring (Figure 3).

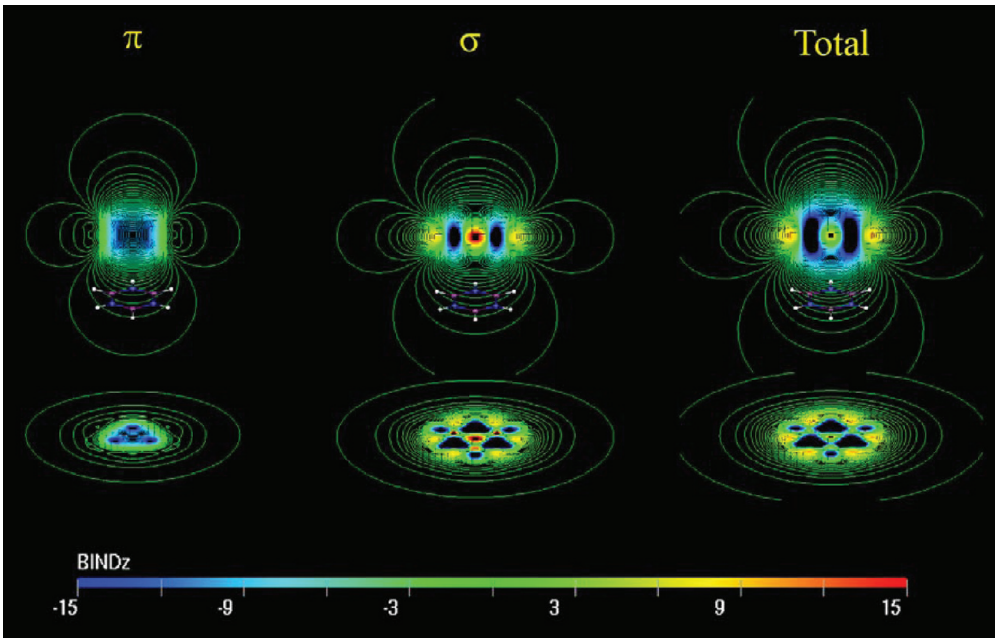

FIGURE 4. Isolines of $B^{ind}{}_z$ in borazine. The scale is given in ppm or μT for an external field of 1 T. $\mathbf{B}^{ind}$ computations were performed at the PW91/IGLO-III level.

Protons are in the shielding region, with the vortexes in close proximity! In contrast, the π-orbital contribution to $\mathbf{B}^{ind}$ shows the typical response of an aromatic system as expected from Pople's model (see Figure 3):

(1) The field lines parallel to the molecular plane lose the shape of the molecular framework and become circles.
(2) No paratropic contributions are found inside the ring. Outside the molecule, the field lines form long-range shielding cones, which indicate a significant contribution of the aromatic ring to the environment.
(3) As suggested by Pople's model, the hydrogen atoms are in the paratropic region of $\mathbf{B}^{ind}$.

It should be noted that our computed field lines correspond even closer to the refinement that Pople's model suggested, for example, in the textbook of Günther.[23] In this model, two ring current loops are considered and two induced circular fields are superposed. The isolines of the π-contributions in Figure 3 show such topology. The graphical representation of the *z*-component of the $\mathbf{B}_\pi{}^{ind}$ field lines, calculated from first principles, supports Pople's model and allows the direct comparison of external magnetic field with the response of the molecule.

Borazine: To Be or Not to Be Aromatic

Similar to benzene, $\mathbf{B}^{ind}$ for borazine shows a long-ranged shielding cone perpendicular to the molecular plane (Figure 4).[24] Note that all atoms and bonds lie in the shielding area of the induced field.

Contrary to benzene, borazine shows two weakly paratropic regions, with one of them inside the ring and the second one enveloping the boron atoms. The σ-orbital contributions to $B^{ind}{}_z$ have a shape which is quite similar to the total $B^{ind}{}_z$ of nonaromatic molecules. The local paramagnetic contributions of the σ-electrons generate a short-range response and a paratropic region in the center of the ring. In contrast, the π-orbital contribution to $B^{ind}{}_z$ shows the typical response of an aromatic system. The field lines parallel to the molecular plane lose the shape of the molecular framework and become circles. No paratropic contributions are found inside the ring. Outside of the molecule, the field lines form long-range shielding cones. The π-contributions are, however, smaller in magnitude than those of benzene, which results in the different topology of the total $B^{ind}{}_z$, in particular in the paratropic area in the ring center. Nevertheless, close to the molecular plane, the σ-contribution is dominating the total response. The shielding cones of borazine on top and bottom, induced by the π-electrons, are comparable in shape to those of benzene, but they are smaller in magnitude and extension (Figure 4). As σ-electrons are much stronger localized than π-electrons, their local paramagnetic contributions generate a short-range response and a paratropic region in the center of the ring (similar to an antiaromatic response).

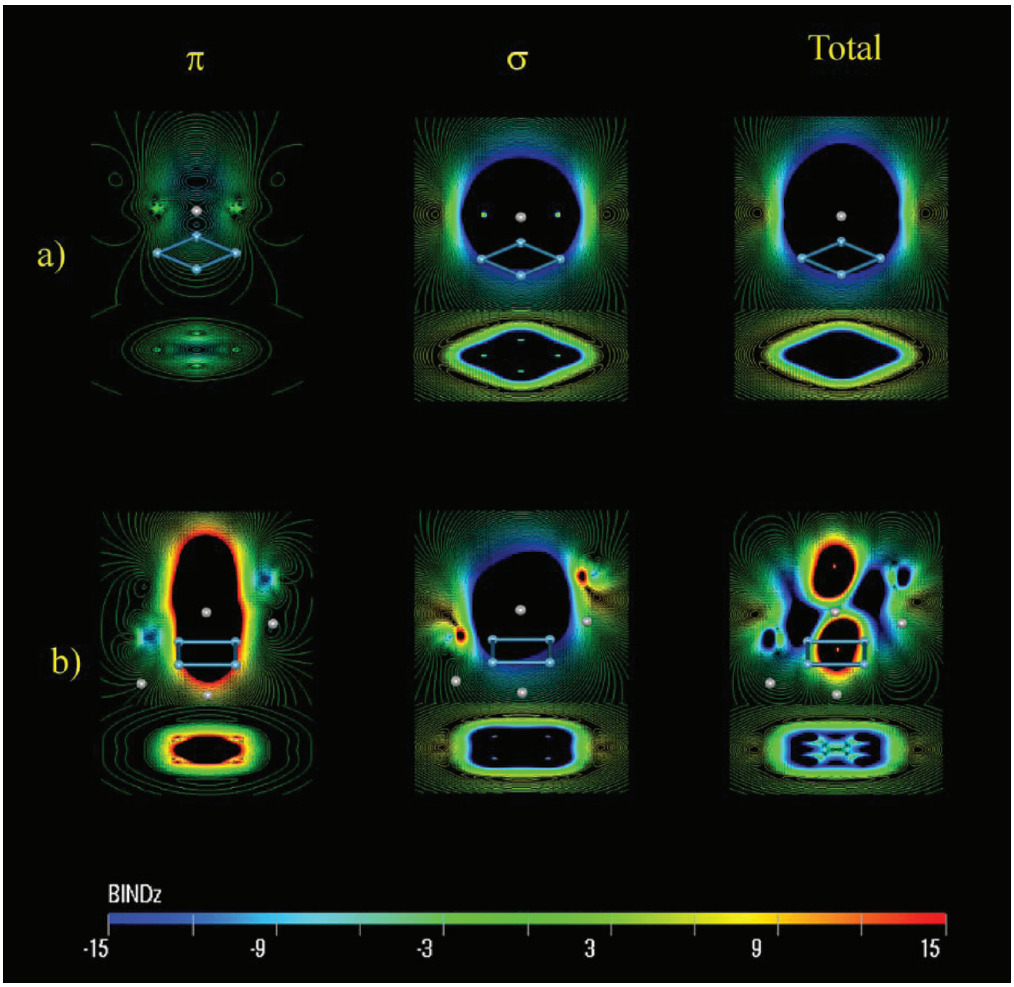

FIGURE 5. Isolines of $B^{ind}{}_z$ in (a) Al_4Li^- and (b) Al_4Li_4. The scale is given in ppm or μT for an external field of 1 T. $\mathbf{B}^{ind}$ computations were performed at the PW91/IGLO-II level.

So, is borazine aromatic? Our results show that the electronic system of borazine is not as homogeneous as that of benzene. The electronegativity difference between B and N has an impact to the chemical bonding pattern and on electron delocalization. Due to the stronger varying potential, $\mathbf{B}^{ind}$ is weaker than that of benzene, but pronounced and long-ranged.

The B^{ind} Analysis Applied to All-Metal Aromatic Systems

Stability based on aromaticity had not been confirmed for any metallic moiety until Li et al. published their seminal paper entitled *"Observation of all-metal aromatic molecules"*.[25] A series of compounds consisting of a square planar Al_4^{2-}, face-capped by an M^+ cation (M = Li, Na, Cu), was produced by laser vaporization, and their electronic spectra were obtained using negative ion photoelectron spectroscopy. Li et al. found that theoretical vertical detachment energies of the pyramidal structures are in excellent agreement with the experimental spectra, thereby suggesting that C_{4v} structures are the global minima for the MAl_4^- species.[25]

Ab initio calculations show that Al_4^{2-} has two electrons residing in a π-orbital, satisfying the Hückel rule for aromatic compounds. Li et al. concluded that this π-orbital holds *"the key to understanding the structure and bonding of MAl_4^- species."*[25] However, electron delocalization in Al_4^{2-} is not so simple. There are two delocalized σ-bonding orbitals (HOMO-1 and HOMO-2) spread across all four aluminum atoms. Therefore, the stability of Al_4^{2-} has been ascribed to its doubly aromatic behavior (π- and σ-aromaticity), which is different from hydrocarbon aromatic molecules.[26]

In 2003, Kuznetsov et al. proposed that the Al_4^{4-} fragment would be a good candidate to be the first antiaromatic all-metal system: if two additional electrons enter the π-system, Al_4^{4-} will be antiaromatic within Hückel theory.[27] They stated that the deviation from an equilateral square ring

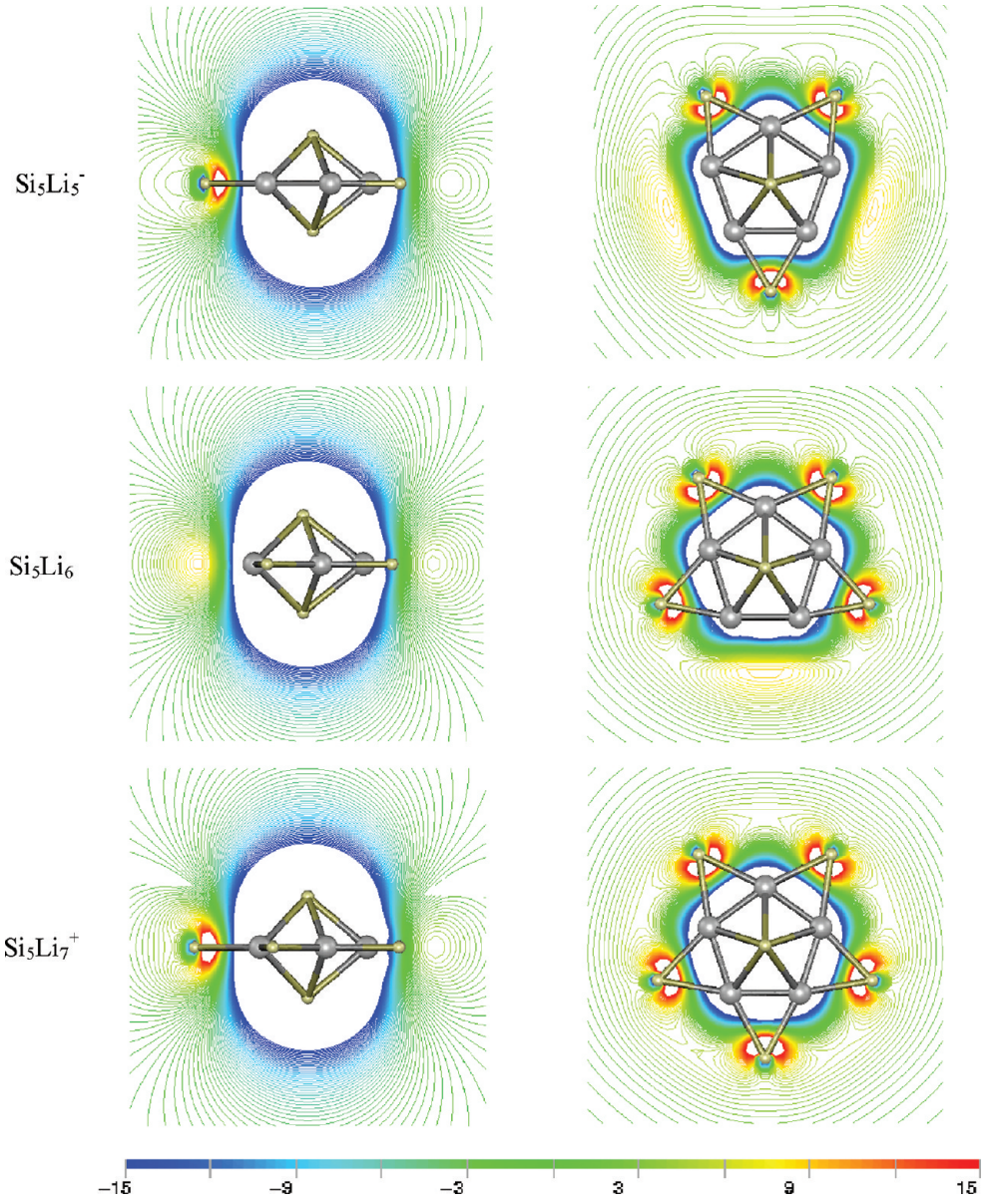

FIGURE 6. Isolines of B^{ind}_z in silicon−lithium stars. The scale is given in ppm or μT for an external field of 1 T. $\mathbf{B}^{ind}$ computations were performed at the PW91/IGLO-II level.

confirms that the compound is antiaromatic. In the same year, Chen et al. argued that the $Al_4Li_3^-$ species is *aromatic* rather than antiaromatic, due to the predominating effects of σ-aromaticity over π-antiaromaticity.[28] This lively discussion has been reviewed by Boldyrev et al.[29]

Cognizant of the difficulties in assigning an aromatic or antiaromatic character to these clusters, we nevertheless tried to improve our understanding of electron delocalization of Al_4^{2-} and Al_4^{4-} using the $\mathbf{B}^{ind}$.[30] We computed the contributions of the π-electrons and of the σ-electrons to the magnetic field individually. With the full magnetic response of the cluster, it is easier to distinguish local effects of the Li ions from those of the Al_4^{n-} clusters, and a more detailed interpretation of the results is possible.

It is not straightforward to separate the magnetic response of planar Al_4^{2-} and Al_4^{4-} clusters into σ- and π-contributions. While for hydrocarbons it is clear that the stabilization of planar rings is due to the π-electrons and Hückel theory is applicable in a straightforward way, for metal clusters the situation is not so simple. For Al_4Li^-, both σ- and π-systems, show a large degree of delocalization, which is a result of the small number of electrons in both electronic subsystems and the ring topology, which favors delocalized electrons, contrary to the results obtained for benzene.

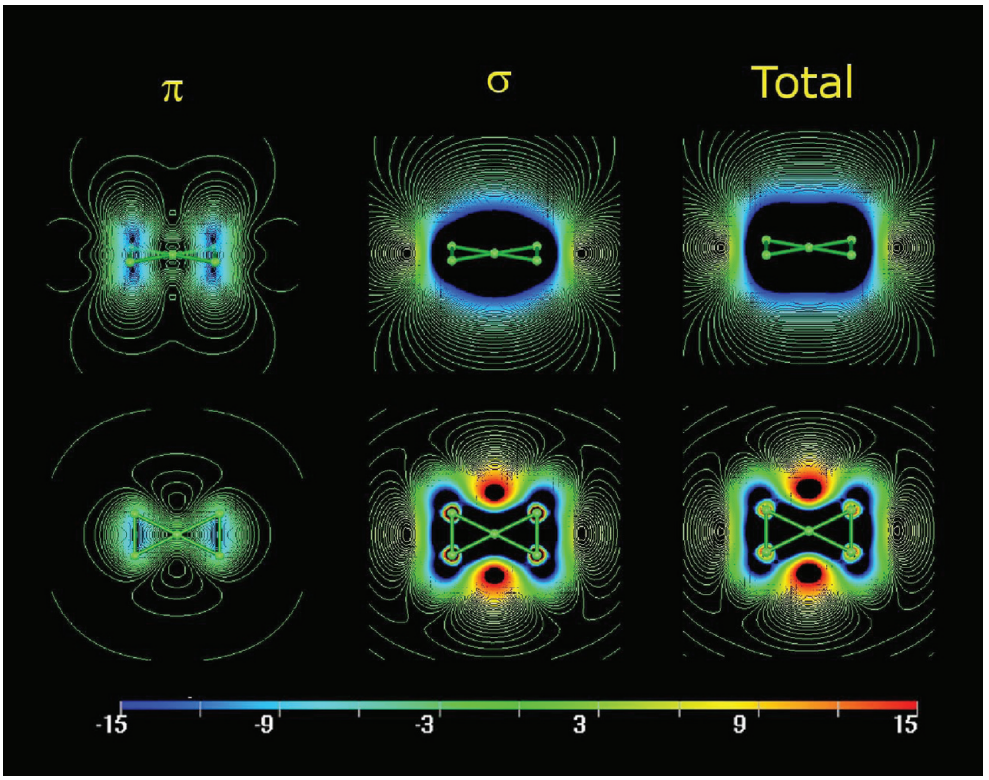

FIGURE 7. Isolines of B^{ind}_z in C_5^{2-}. The scale is given in ppm or μT for an external field of 1 T. $\mathbf{B}^{ind}$ computations were performed at the PW91/IGLO-III level.

For Al_4Li_4, the situation is not that clear. The shielding cone of the molecule on top and bottom, induced by the π-electrons, is comparable to that of cyclobutadiene, though smaller in magnitude and perturbed by the Li ions (See Figure 5). Closer to the ring plane and at positions far from the ring center, however, the response is diatropic and similar to that of an aromatic hydrocarbon. It is therefore difficult to make a final statement as to whether Al_4^{4-} should be called aromatic or antiaromatic. The NICS or B^{ind}_z isolines or isosurfaces give us important (but still partial) insight into electron delocalization. It is, however, clear that σ- and π-components of Al_4^{4-} show an opposite response, so in this sense we could name it a *bitropic* behavior, in agreement with the conflicting aromaticity concept introduced by Boldyrev and Wang.[29]

Molecular Stars

In 2009, we explored in detail the potential energy surfaces of the $Si_5Li_n^{6-n}$ ($n = 5-7$) systems.[31] We found that it is feasible to design three-dimensional starlike silicon structures using the appropriate ligands. The global minimum structure for $Si_5Li_7^+$ has a perfect seven-peak starlike structure. These clusters comprise, essentially, the Si_5^{6-} ring interacting with lithium cations. The ionic character of the Si−Li interactions induces the formation of a bridged structure. Figure 6 depicts the contour lines of B^{ind}_z for $Si_5Li_5^-$, Si_5Li_6, and $Si_5Li_7^+$. The shielding cones of the silicon clusters above and below the ring are comparable in shape to those of benzene, even though they are larger in magnitude and extension. Around the σ-framework of Si_5^{6-}, there are five paratropic regions (one at each of the sides of the pentagon). This behavior does not depend on the number of cations and is a clear consequence of the strong electron delocalization. The B^{ind}_z value at the center of the Si_5 ring (let us call it $B^{ind}_z(0)$ in analogy to NICS(0)) in $Si_5Li_7^+$ (−44 ppm) is approximately 3 times larger than that in benzene (−15.9 ppm). The corresponding value for the D_{5h} $Si_5H_5^-$ structure is only −13.7 ppm; thus, it is apparent that substitution of hydrogen for lithium intensifies electron delocalization into the Si ring. Notice that $B^{ind}_z(0)$ increases from $Si_5Li_7^+$ (−56.8 ppm) to $Si_5Li_5^-$ (−44.7 ppm). In summary, the magnetic properties show that the significant electron delocalization enhances the stability of the structures proposed here and render them amenable to experimental detection.

Planar Tetracoordinate Carbon Atoms

In 1970, Hoffmann, Alder, and Wilcox suggested rules to stabilize molecules with a planar tetracoordinate carbon

(ptC).[32] Collins et al.'s systematic computational investigation identified the first molecules with ptC minima in 1976.[33] Motivated by this interesting idea, several groups, including us,[34−39] have successfully suggested and, in some cases, experimentally characterized molecules containing ptC atoms or even having a higher coordination.

In 2003, the first family of molecules based on a C_5^{2-} skeleton that successfully stabilized a ptC only by electronic factors was reported.[34] One year later, the magnetic properties of these compounds were studied, giving particular attention to the NICS and $\mathbf{B}^{ind}$ of C_5^{2-}.[39] As it can be seen in Figure 7, strong diatropic contributions are observed around the three-membered rings. This trend is a clear electron delocalization consequence. Note that the most important contribution to the $B^{ind}{}_z$ comes from the σ-framework. The π-system slightly influences to the total magnetic response. In summary, the magnetic properties show that the C_5^{2-} dianion is highly delocalized.

In 2005, we studied a series of cyclic hydrocarbons containing a planar tetracoordinate carbon atom.[36] To rationalize the electronic factors contributing to the stability of these molecules, an analysis of the molecular orbitals and $\mathbf{B}^{ind}$ was presented. Figure 8 shows the $B^{ind}{}_z$ isolines of such cyclic hydrocarbons. All molecules have strong diatropic contributions (in blue) inside of the three-membered rings. The five- and eight-membered ring shows an aromatic response for the $(4n + 2)\pi$-electrons species, while an antiaromatic response for the 8 π-electron cycles $C_8H_3^-$ and C_9H_4 is observed. Note that C_7H_2 shows a weak paratropic contribution inside the ring. For C_7H_2 and $C_{10}H_5^-$, the shielding regions (given in blue) are around the molecule, while deshielding ones are further outside (given in red). The opposite situation is observed in 8 π-electron molecules.

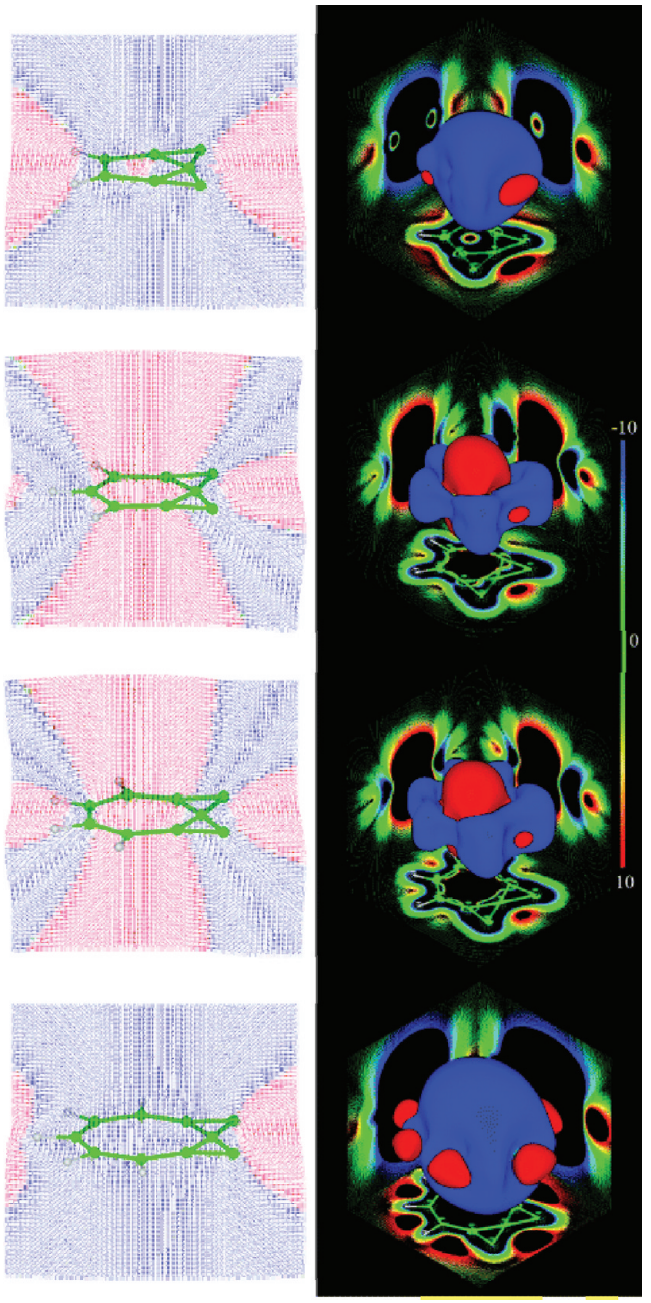

FIGURE 8. Left: $\mathbf{B}^{ind}$ of an external field in *z*-direction to molecules located in the *xy* plane. Diatropic and paratropic contributions are given in blue and red, respectively. Right: Isosurfaces of $B^{ind}{}_z$ (9.0 μT) and $\mathbf{B}^{ext}$ = 1.0 T perpendicular to the molecular plane. Blue and red indicate shielding and deshielding areas, respectively. $\mathbf{B}^{ind}$ computations were performed at the PW91/IGLO-II level.

Planar Hypercoordinate Atoms

Eleven years ago, Exner and Schleyer suggested that CB_6^{2-} could adopt a structure containing a planar hexacoordinate carbon atom. Immediately, this divining structure caught the attention of the chemical community. In 2008, Averkiev and co-workers observed a highly stable CB_6^{2-} cluster during laser vaporization experiments.[40] Using photoelectron spectroscopy (PES) and ab initio calculations, the authors demonstrated that the D_{6h} form is not the global minimum structure. A similar situation is found for CB_7^-.[41]

We surveyed a series of local minima with hypercoordinate group 14 elements at the center of *n*-membered boron rings (*n* = 6, 7, 8, 9, and 10; see Figure 9).[42] Boron clusters utilize extensively delocalized bonds readily. Due to its electron deficient character and propensity for deltahedral bonding, boron is intrinsically suitable for designing ring systems containing hypercoordinate elements. The strategy for designing boron rings with planar hypercoordinate elements is as follows: First, the cyclic boron ligand must have

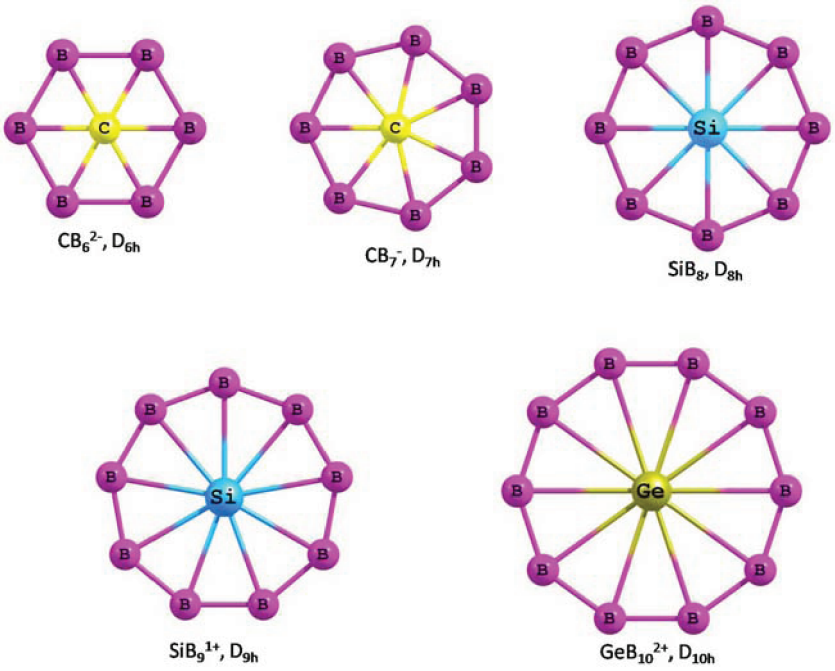

FIGURE 9. Optimized geometries of planar boron wheels containing a planar hypercoordinate group 14 element.

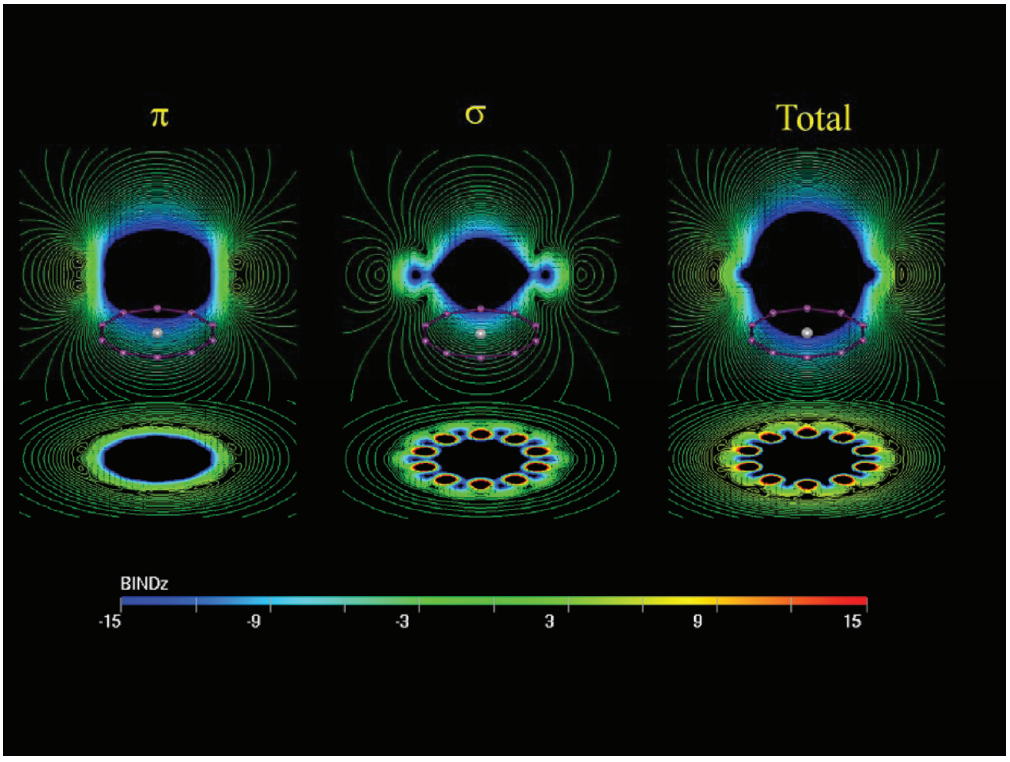

FIGURE 10. Contour lines of $B^{ind}{}_z$ of GeB_{10}^{2+}. $\mathbf{B}^{ext} = 1$ T. $\mathbf{B}^{ind}$ computations were performed at the PW91/IGLO-III level.

the right size to accommodate a group 14 atom inside without steric repulsion. Second, the electronic structure of the molecule is adjusted by varying charge so that the molecule has six π- and six radial- electrons.

The appreciable delocalization of both π- and radial-MOs of these hypercoordinate species can be described in terms of $\mathbf{B}^{ind}$. In this case, the σ- and π-separated $B^{ind}{}_z$ of D_{10h} GeB_{10}^{2+} are plotted in Figure 10. The total response is

strongly diatropic (shown in blue) inside the main ring. However, both σ- and π-components of GeB_{10}^{2+} contribute strongly, indicating a doubly aromatic character.

Recently, the groups of Wang and Boldyrev detected B_{19}^- by mass spectrometry and gas-phase photoelectron spectroscopy experiments and explained its bonding system.[43] This cluster has a nearly circular planar structure, with two π-electrons delocalized over the B_6 ring and another 10 π-electrons shared between the B_6 and B_{13} rings. We found that bonds between the B_{19}^- cluster's inner B_6 ring and outer B_{13} ring constantly break and reform via a low-energy transition state in such a way that the pentagon-shaped hub and the B_{13} wheel rotate in opposite directions.[44]

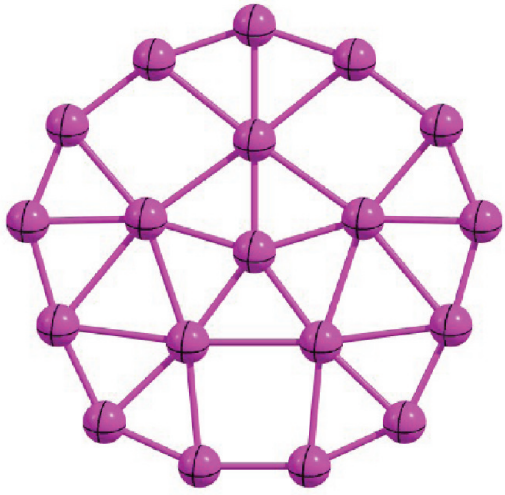

B_{19}^-

Figure 11 shows the B^{ind}_z isolines of **1**. The total magnetic response shows a long-range shielding cone perpendicular to the molecular plane. This cone is even more intense to that observed in benzene: the inner ring lies in the strong shielding area (approximately −100 ppm, compared to −20 ppm in benzene) of the induced field. The local diamagnetic contributions of the σ-electrons generate a long-range response and a diatropic (shielding) region in the pentagonal ring. Furthermore, the π-orbital contribution shows the typical response of an aromatic system. Similar as in benzene, the field lines parallel to the molecular plane lose the shape of the molecular framework and become circles. No paratropic contributions are found inside the ring. Outside of the molecule the field lines form long-range cones (shielding cones). The π-contributions are, however, smaller in magnitude than those of the σ-skeleton, which results in a strong total response. So, similar to Al_4^{2-}, the contribution of the π-system in B_{19}^- is smaller to the σ-system, but it is still important for the total response. In this sense, B_{19}^- is a double aromatic system. During the rotation the changes in σ- and π-aromaticity are negligible. This is a big difference to classical organic systems, as coronene, where the rotation of the inner ring modifies drastically the overlap of the π system and obviously aromaticity. However, we found a similar fluxional and delocalization situation in B_{13}^+ and other boron clusters.[45]

Warnings

We have shown that the electron delocalization degree in the planar hydrogen-bonded HF cyclic trimer is very low.[46] This result is in agreement with that obtained using GIMIC[47] and is opposite to the Rehaman et al. suggestion.[48] Our results show a clear limitation of the NICS index when a strong anisotropy is exhibited and suggest that the NICS values should be used carefully to discuss aromaticity in systems without an important overlap of p_z orbitals that produce the π clouds. In view of the fact that the NICS index is extensively used by computationally and theoretically oriented experimental chemists, this is an important warning. Our results are also in line with the Lazzeretti comments, who mentioned that the analyses based on average values imply a loss of information, and thus criteria for diatropicity and aromaticity should be established in terms of the out-of-plane component of magnetic tensors.[11] Our conclusion is that one needs to be cautious regarding an interpretation of the NICS index.

On the other hand, can relativistic effects modify the NICS and the $\mathbf{B}^{ind}$ values? We evaluated the relativistic corrections incorporated via the zeroth-order regular approximation to the calculations of NICS and $\mathbf{B}^{ind}$ in the E_{12}^{2-} spherenes (E = Ge, Sn, Pb). We found that both electron delocalization descriptors are strongly affected by the relativistic corrections. For instance, for plumbaspherene, the difference in values from the nonrelativistic to the relativity-included calculations is almost 40 ppm! Our results show that the changes observed in the NICS and $\mathbf{B}^{ind}$ values in the title cages are a consequence of the treatment of the relativistic effects. If these effects are included as scalar or spin−orbit calculations, then we can establish the next trend: Ge_{12}^{2-} is a nonaromatic species, Sn_{12}^{2-} is a low aromatic species, and Pb_{12}^{2-} is strongly aromatic, according to calculated NICS and $\mathbf{B}^{ind}$ values. Thus, any prediction of electron delocalization in molecules containing heavy elements without considering an adequate treatment for relativistic effects may lead to an erroneous chemical interpretation.

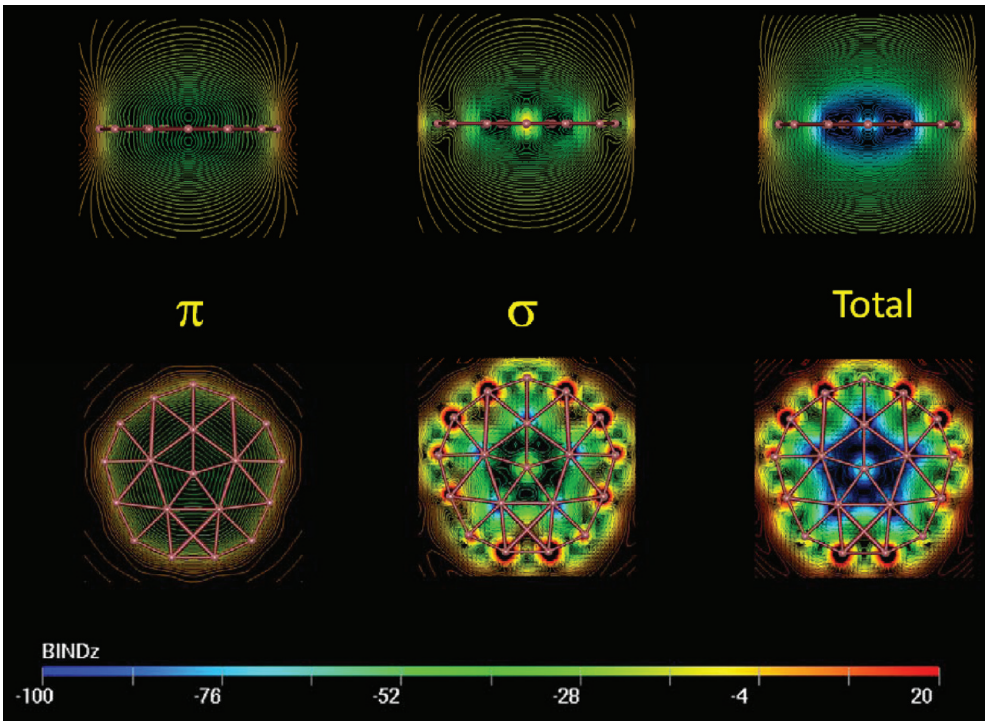

FIGURE 11. Contour lines of B^{ind}_z of B_{19}^-. $\mathbf{B}^{ext} = 1$ T. $\mathbf{B}^{ind}$ computations were performed at the PW91/IGLO-III level.

Conclusions

Planar molecules gain additional stability by forming a two-dimensional system of delocalized electrons, similar to the semimetallic π-electrons in graphene. This electron delocalization is often synonymously used with the term aromaticity. A delocalized electron system is sensitive to an external magnetic field and shows a typical, appreciable response, an induced magnetic field with a particular long-range. Its shape reflects the size and strength of the system of delocalized electrons and can have a sizable influence on neighboring molecules.

Quantitatively, the induced magnetic field has contributions from the entire electronic system of a molecule, but at long ranges the contributions arising from the delocalized electronic (π) system dominate. $\mathbf{B}^{ind}$ can only indirectly be confirmed in experiment, for example, through intermolecular contributions to NMR chemical shifts.

We have shown that the calculation of $\mathbf{B}^{ind}$ is a meaningful analysis tool for any planar organic or inorganic system, as it corresponds to the intuitive Pople model for explaining the anomalous proton chemical shifts in aromatic molecules. Indeed, aromatic, antiaromatic, or nonaromatic molecules show a different response to an external field; that is, they are reducing, enforcing, or not affecting the external field at long-range. $\mathbf{B}^{ind}$ can be dissected into different orbital contributions in the same way as NICS or the shielding function, which is useful for the analysis of planar densely packed systems with strong contributions directly on top of individual atoms, as, for example, for systems containing highly coordinated atoms as planar tetra- or pentacoordinate carbon or for boron wheels.

Any visual representation of the induced magnetic field (isosurfaces, isolines, vector, etc.) gives meaningful information about electron delocalization. We should finally note that $\mathbf{B}^{ind}$ is a consequence of 2D electron delolcalization, as any other magnetic index (NICS, ARCS, HOMA, ACID, etc.). Interpretation of $\mathbf{B}^{ind}$ in terms of aromaticity should be done with extreme care, since as any interpretation it has a degree of subjectivity.

We are grateful to many colleagues for their collaboration in this project: Alberto Vela from Cinvestav (Mexico), Keigo Ito, and Paul Schleyer from University of Georgia (USA), Clémence Corminboeuf from EPFL (Switzerland), Vladimir Malkin and Olga Malkina from Slovak Academy of Sciences (Slovakia), Nancy Perez-Peralta and Gerardo Martínez-Guajardo from Universidad de Guanajuato (Mexico), Gotthard Seifert from Technische Universität Dresden (Germany), Miquel Sola from University of Girona, and Juan Carlos Santos, William Tiznado, and Eduardo Chamorro from Universidad Andres Bello (Chile). This work was supported in Guanajuato by Conacyt (Grant 57892) and DAIP. R.I. thanks Conacyt for the Ph.D. fellowship.

BIOGRAPHICAL INFORMATION

Rafael Islas was born in Ocotlán, Mexico. He received a Chemistry degree from Universidad de Guanajuato in 2007. In the same year, he received the National Prize for the best bachelor thesis in Chemistry in Mexico. He received a Ph.D. in 2011 in the Department of Chemistry of Universidad de Guanajuato in Mexico (supervisor Gabriel Merino).

Thomas Heine (born 1970 in Germany) graduated in 1995 in Theoretical Physics (TU Clausthal, Germany) and obtained his Ph.D. in Theoretical Physics at TU Dresden, Germany, in 1999, working with Gotthard Seifert on the calculation of NMR patterns of fullerenes. Several pre- and postdoctoral stages introduced him into the field of physical and theoretical chemistry. In 2006, he obtained the Venia Legendi in Physical Chemistry from TU Dresden. He was appointed as Associate Professor of Theoretical Physics at Jacobs University Bremen, Germany, in 2008. He currently works on the development of density functional theory related methods, metal–organic frameworks, and aromaticity, and on the electronic properties of inorganic nanostructures.

Gabriel Merino was born in 1975 in Puebla, Mexico. He received a B.S. in chemistry in 1997 from Universidad de las Americas-Puebla and a Ph.D. in 2003 from Cinvestav (with Alberto Vela). He then did postdoctoral research at TU Dresden with Gotthard Seifert. Professor Merino joined the Department of Chemistry at Universidad de Guanajuato in 2005, and he became Full Professor in 2008. He has also served as Visiting Professor at Cornell University in 2006 (Roald Hoffmann) and at University of Basque Country in 2011 (Jesus Ugalde). His research is driven by puzzling bonding questions, designing and predicting new molecular systems.

FOOTNOTES

*E-mail: gmerino@quijote.ugto.mx (G.M.); t.heine@jacobs-university.de (T.H.).

REFERENCES

1 Frenking, G.; Krapp, A. Unicorns in the world of chemical bonding models. *J. Comput. Chem.* **2007**, *28*, 15–24.

2 Minkin, V. I. Glossary of Terms used in Theoretical Organic Chemistry. *Pure Appl. Chem.* **1999**, *71*, 1919–1981.

3 Schleyer, P. v. R. Introduction: Aromaticity. *Chem. Rev.* **2001**, *101*, 1115–1117.

4 Schleyer, P. v. R. Introduction: Delocalization - Pi and Sigma. *Chem. Rev.* **2005**, *105*, 3433–3435.

5 Chen, Z. F.; Wannere, C. S.; Corminboeuf, C.; Puchta, R.; Schleyer, P. v. R. Nucleus-Independent Chemical Shifts (NICS) as an Aromaticity Criterion. *Chem. Rev.* **2005**, *105*, 3842–3888.

6 Schleyer, P. v. R.; Maerker, C.; Dransfeld, A.; Jiao, H. J.; Hommes, v. E. N. J. R. Nucleus-Independent Chemical Shifts: A Simple and Efficient Aromaticity Probe. *J. Am. Chem. Soc.* **1996**, *118*, 6317–6318.

7 Steinmann, S. N.; Jana, D. F.; Wu, J. I. C.; Schleyer, P. v. R.; Mo, Y. R.; Corminboeuf, C. Direct Assessment of Electron Delocalization Using NMR Chemical Shifts. *Angew. Chem., Int. Ed.* **2009**, *48*, 9828–9833.

8 Juselius, J.; Sundholm, D. Ab Initio Determination of the Induced Ring Current in Aromatic Molecules. *Phys. Chem. Chem. Phys.* **1999**, *1*, 3429–3435.

9 Gomes, J.; Mallion, R. B. Aromaticity and Ring Currents. *Chem. Rev.* **2001**, *101*, 1349–1383.

10 Steiner, E.; Fowler, P. W. Patterns of ring currents in conjugated molecules: A few-electron model based on orbital contributions. *J. Phys. Chem. A* **2001**, *105*, 9553–9562.

11 Lazzeretti, P. Ring Currents. *Prog. Nucl. Magn. Reson. Spectrosc.* **2000**, *36*, 1–88.

12 Fleischer, U.; Kutzelnigg, W.; Lazzeretti, P.; Muhlenkamp, V. Iglo Study of Benzene and some of its Isomers and Related Molecules -Search for Evidence of the Rng Current Model. *J. Am. Chem. Soc.* **1994**, *116*, 5298–5306.

13 Hückel, E. Zur Quantentheorie der Doppelbindung. *Z. Phys.* **1930**, *60*, 423.

14 Pople, J. A. Proton Magnetic Resonance of Hydrocarbons. *J. Chem. Phys.* **1956**, *24*, 1111–1112.

15 Merino, G.; Heine, T.; Seifert, G. The Induced Magnetic Field in Cyclic Molecules. *Chem.—Eur. J.* **2004**, *10*, 4367–4371.

16 Heine, T.; Islas, R.; Merino, G. Sigma and Pi Contributions to the Induced Magnetic Field: Indicators for the Mobility of Electrons in Molecules. *J. Comput. Chem.* **2007**, *28*, 302–309.

17 Heine, T.; Corminboeuf, C.; Seifert, G. The Magnetic Shielding Function of Molecules and Pi-electron Delocalization. *Chem. Rev.* **2005**, *105*, 3889–3910.

18 Corminboeuf, C.; Heine, T.; Seifert, G.; Schleyer, P. v. R.; Weber, W. Induced Magnetic Fields in Aromatic [n]-Annulenes —Interpretation of NICS Tensor Components. *Phys. Chem. Chem. Phys.* **2004**; *6*, 273—276.

19 Schleyer, P. v. R.; Manoharan, M.; Wang, Z. X.; Kiran, B.; Jiao, H. J.; Puchta, R.; Hommes, v. E. N. J. R. Dissected Nucleus-Independent Chemical Shift Analysis of Pi-aromaticity and Antiaromaticity. *Org. Lett.* **2001**, *3*, 2465–2468.

20 Faglioni, F.; Ligabue, A.; Pelloni, S.; Soncini, A.; Viglione, R. G.; Ferraro, M. B.; Zanasi, R.; Lazzeretti, P. Why Downfield Proton Chemical Shifts are not Reliable Aromaticity Indicators. *Org. Lett.* **2005**, *7*, 3457–3460.

21 Wannere, C. S.; Corminboeuf, C.; Allen, W. D.; Schaefer, H. F.; Schleyer, P. v. R. Downfield Proton Chemical Shifts are not Reliable Aromaticity Indicators. *Org. Lett.* **2005**, *7*, 1457–1460.

22 Viglione, R. G.; Zanasi, R.; Lazzeretti, P. Are Ring Currents still Useful to Rationalize the Benzene Proton Magnetic Shielding? *Org. Lett.* **2004**, *6*, 2265–2267.

23 Günther, H. *NMR Spectroscopy: Basic Principles, Concepts, and Applications in Chemistry*, 2nd ed.; Wiley: Chichester; New York, 1995.

24 Islas, R.; Chamorro, E.; Robles, J.; Heine, T.; Santos, J. C.; Merino, G. Borazine: to be or not to be Aromatic. *Struct. Chem.* **2007**, *18*, 833–839.

25 Li, X.; Kuznetsov, A. E.; Zhang, H. F.; Boldyrev, A. I.; Wang, L. S. Observation of All-Metal Aromatic Molecules. *Science* **2001**, *291*, 859–861.

26 Kuznetsov, A. E.; Boldyrev, A. I.; Li, X.; Wang, L. S. On the Aromaticity of Square Planar Ga_4^{2-} and In_4^{2-} in gaseous $NaGa_4^-$ and $NaIn_4^-$ clusters. *J. Am. Chem. Soc.* **2001**, *123*, 8825–8831.

27 Kuznetsov, A. E.; Birch, K. A.; Boldyrev, A. I.; Li, X.; Zhai, H. J.; Wang, L. S. All-metal antiaromatic molecule: Rectangular Al_4^{4-} in the $Li_3Al_4^-$ Anion. *Science* **2003**, *300*, 622–625.

28 Chen, Z. F.; Corminboeuf, C.; Heine, T.; Bohmann, J.; Schleyer, P. v. R. Do All-Metal Antiaromatic Clusters Exist? *J. Am. Chem. Soc.* **2003**, *125*, 13930–13931.

29 Boldyrev, A. I.; Wang, L. S. All-Metal Aromaticity and Antiaromaticity. *Chem. Rev.* **2005**, *105*, 3716–3757.

30 Islas, R.; Heine, T.; Merino, G. Structure and Electron Delocalization in Al_4^{2-} and Al_4^{4-}. *J. Chem. Theory Comput.* **2007**, *3*, 775–781.

31 Tiznado, W.; Perez-Peralta, N.; Islas, R.; Toro-Labbe, A.; Ugalde, J. M.; Merino, G. Designing 3-D Molecular Stars. *J. Am. Chem. Soc.* **2009**, *131*, 9426–9431.

32 Hoffmann, R.; Alder, R. W.; Wilcox, C. F. Planar Tetracoordinate Carbon. *J. Am. Chem. Soc.* **1970**, *92*, 4992.

33 Collins, J. B.; Dill, J. D.; Jemmis, E. D.; Apeloig, Y.; Schleyer, P. v. R.; Seeger, R.; Pople, J. A. Stabilization of Planar Tetracoordinate Carbon. *J. Am. Chem. Soc.* **1976**, *98*, 5419–5427.

34 Merino, G.; Mendez-Rojas, M. A.; Vela, A. $C_5M_{2-n}^{n-}$ (M = Li, Na, K, and n = 0, 1, 2). A New Family of Molecules containing Planar Tetracoordinate Carbons. *J. Am. Chem. Soc.* **2003**, *125*, 6026–6027.

35 Pancharatna, P. D.; Mendez-Rojas, M. A.; Merino, G.; Vela, A.; Hoffmann, R. Planar Tetracoordinate Carbon in Extended Systems. *J. Am. Chem. Soc.* **2004**, *126*, 15309–15315.

36 Perez, N.; Heine, T.; Barthel, R.; Seifert, G.; Vela, A.; Mendez-Rojas, M. A.; Merino, G. Planar Tetracoordinate Carbons in Cyclic Hydrocarbons. *Org. Lett.* **2005**, *7*, 1509–1512.

37 Merino, G.; Mendez-Rojas, M. A.; Vela, A.; Heine, T. Recent Advances in Planar Tetracoordinate Carbon Chemistry. *J. Comput. Chem.* **2007**, *28*, 362–372.

38 Perez-Peralta, N.; Sanchez, M.; Martin-Polo, J.; Islas, R.; Vela, A.; Merino, G. Planar Tetracoordinate Carbons in Cyclic Semisaturated Hydrocarbons. *J. Org. Chem.* **2008**, *73*, 7037–7044.

39 Merino, G.; Mendez-Rojas, M. A.; Beltraan, H. I.; Corminboeuf, C.; Heine, T.; Vela, A. Theoretical Analysis of the Smallest Carbon Cluster containing a Planar Tetracoordinate Carbon. *J. Am. Chem. Soc.* **2004**, *126*, 16160–16169.

40 Averkiev, B. B.; Zubarev, D. Y.; Wang, L. M.; Huang, W.; Wang, L. S.; Boldyrev, A. I. Carbon avoids Hypercoordination in CB_6^-, CB_6^{2-}, and $C_2B_5^-$ Planar Carbon-Boron Clusters. *J. Am. Chem. Soc.* **2008**, *130*, 9248–9250.

41 Wang, L. M.; Huang, W.; Averkiev, B. B.; Boldyrev, A. I.; Wang, L. S. CB7-: Experimental and Theoretical Evidence against Hypercoordinate Planar Carbon. *Angew. Chem., Int. Ed.* **2007**, *46*, 4550–4553.

42 Islas, R.; Heine, T.; Ito, K.; Schleyer, P. v. R.; Merino, G. Boron Rings enclosing Planar Hypercoordinate Group 14 elements. *J. Am. Chem. Soc.* **2007**, *129*, 14767–14774.

43 Huang, W.; Sergeeva, A. P.; Zhai, H. J.; Averkiev, B. B.; Wang, L. S.; Boldyrev, A. I. A Concentric Planar Doubly Pi-Aromatic B_{19}^- cluster. *Nat. Chem.* **2010**, *2*, 202–206.

44 Jimenez-Halla, J.; Islas, R.; Heine, T.; Merino, G. B_{19}^-: An Aromatic Wankel Motor. *Angew. Chem., Int. Ed.* **2010**, *49*, 5668–5671.

45 Martinez-Guajardo, G.; Sergeeva, A. P.; Boldyrev, A. I.; Heine, T.; Ugalde, J. M.; Merino, G. Unravelling Phenomenon of Internal Rotation in B_{13}^+ through Chemical Bonding Analysis. *Chem. Commun.* **2011**, *47*, 6242–6244.

46 Islas, R.; Martinez-Guajardo, G.; Jimenez-Halla, J. O. C.; Sola, M.; Merino, G. Not All That Has a Negative NICS Is Aromatic: The Case of the H-Bonded Cyclic Trimer of HF. *J. Chem. Theory Comput.* **2010**, *6*, 1131–1135.

47 Lin, Y. C.; Sundholm, D.; Juselius, J. On the Aromaticity of the Planar Hydrogen-bonded $(HF)_3$ Trimer. *J. Chem. Theory Comput.* **2006**, *2*, 761–764.

48 Rehaman, A.; Datta, A.; Mallajosyula, S. S.; Pati, S. K. Quantifying Aromaticity at the Molecular and Supramolecular Limits: Comparing Homonuclear, Heteronuclear, and H-Bonded Systems. *J. Chem. Theory Comput.* **2006**, *2*, 30–36.